ADVANCED MATERIALS INTERFACES
www.advmatinterfaces.de

Surface Cleaning of 2D Materials: Boron Nitride Nanosheets (BNNS) and Exfoliated Graphite Nanoplatelets (GNP)

*Valentina Guerra and Tony McNally**

Surface impurities such as water and surfactants can significantly affect the properties of 2D materials. They disrupt the 2D material lattice structure and surface chemistry and also promote electron and phonon scattering. Strategies to clean the surfaces of 2D materials are therefore critical to achieving optimal properties. Boron nitride nanosheets (BNNS) and exfoliated graphite nanoplatelets (GNP) are treated using three procedures: washing with ethanol, water-assisted freeze-drying, and freeze-drying without addition of water in an attempt to remove two impurities—water and an ionic surfactant (sodium cholate, SC). There is total removal of water from BNNS when the starting material is treated using either freeze drying method whereas some water (≈40%) and traces of ethanol are detected in BNNS when washed with ethanol. It is not possible to exclude the presence of SC on BNNS and GNP post treatment; however, the relatively high amount of sodium (from SC) in the samples after freeze-drying suggests the process contributed to the separation of BNNS and GNP aggregates. The BNNS flakes separate when washed with ethanol or freeze-dried in the absence of water. The crystalline structure of BNNS and GNP is retained post treatments. This approach provides a route to cleaning and separating 2D materials.

1. Introduction

Contamination on the surface of 2D materials, such as boron nitride nanosheets (BNNS) and the graphene family of materials is detrimental to their intrinsic transport properties (e.g., thermal, electrical conduction) as they induce electron and phonon scattering, reducing electrical and thermal conduction.[1–4] Different approaches have been adopted to clean the surface of 2D materials from surface contaminants and impurities using methodologies such as electrical current annealing,[5] thermal annealing/desorption,[6–12] washing with water, acids, bases, ethanol,[12–14] plasma treatment,[13] and etching of metals.[15] Electrical annealing is effective at cleaning the surfaces of 2D materials; however, it is very limited in that it can only treat small sample areas (few micrometer square).[5] Thermal annealing proved to be the most effective at removing the impurities from the surface of 2D materials; however, there are serious concerns with regard degradation of the 2D material as a function of time. Washing with acids/bases are not always desirable as they can alter surface chemistry and their use may negatively impact the environment.[15] The etching of metals procedure is too laborious and not readily suitable for large-scale applications.

Almost without exception the top-down production of 2D materials requires the use of surfactants or dispersants (e.g., water, ionic liquids) to assist the exfoliation of some bulk material. By way of example, the pretreatment of BNNS and exfoliated graphite nanoplatelets (GNP) studied here contain trace water and surfactant (sodium cholate, SC),[16,17] mainly introduced during the exfoliation of the corresponding bulk materials (i.e., boron nitride and graphite) in a high pressure homogenizer.[18] Specifically, three cleaning procedures were adopted in an attempt to remove impurities (i.e., water and SC) from the surfaces of BNNS and GNP, namely washing with ethanol, water assisted-freeze drying, and freeze drying without addition of water. Ethanol (EtOH) was utilized as it can wash water away from the surface of the BNNS and GNP and interact with the ionic surfactant SC thus being removed. The freeze drying process was selected as the sublimation of iced-water from the surface of BNNS and GNP would ideally remove water and exfoliate the 2D material further.[19–23] Indeed, when ice sublimates, the layers and flakes surrounded by ice are pulled apart. Two specific procedures for freeze drying were realized; FD-(i) – freezing of a dispersion of BNNS or GNP in water in liquid nitrogen followed by freeze drying and FD-(ii) – freezing in liquid nitrogen of the as received BNNS or GNP powder followed by freeze drying. The latter was performed on the basis that the water present as impurity in the BNNS and GNP samples would be sufficient at creating an ice pattern cutting through the layered structure

V. Guerra, Prof. T. McNally
International Institute for Nanocomposite Manufacturing (IINM)
WMG
University of Warwick
Warwick CV4 7AL, UK
E-mail: t.mcnally@warwick.ac.uk

The ORCID identification number(s) for the author(s) of this article can be found under https://doi.org/10.1002/admi.202000944.

DOI: 10.1002/admi.202000944

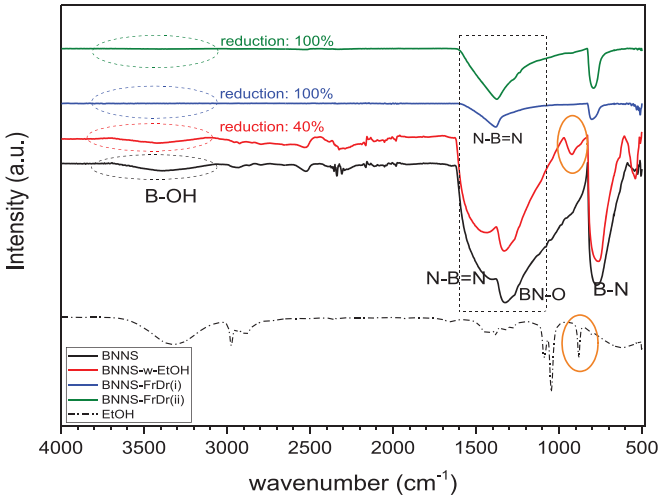

Figure 1. FTIR spectra of BNNS as received (black solid) and after treatment. The spectrum of EtOH was also recorded for comparison with BNNS-w-EtOH.

of the 2D material when freezing without adding any further water, as is normally required in the freeze drying process (method FD-(i)). Further details on each methodology are provided in the Experimental Section.

2. Results and Discussion

The Fourier transform infrared spectroscopy (FTIR) spectra of as received BNNS post-treatment are shown in **Figure 1**. The FTIR of GNP (not shown), showed the peaks related to the oxidized groups were negligible and no accurate calculation could be conducted as the peak areas fell within the error of the measurements.

The presence of the B—OH band at ≈3300 cm^{-1} in the BNNS spectra is derived from water whereas the broad overlapping bands N—B=N/BN—O at ≈1300–1400 cm^{-1}[24] are due to both the presence of water and interactions of BNNS with SC. It is clear that washing with EtOH reduced the water content (B—OH band area decreased by ≈40%), yet the two broad bands for N—B=N/BN—O are still present, indicating that both the water and probably SC were not totally removed. Furthermore, the peak at ≈900 cm^{-1} in the BNNS spectrum is associated with EtOH entrapped in the BNNS, see peak enclosed in red circle in Figure 1.

The two procedures adopted for freeze-drying completely removed water from the BNNS surface as no B—OH and BN—O bands were recorded in the FTIR spectra. The peak from N—B=N at ≈1400 cm^{-1} indicates that BNNS does not contain water, but it is not possible to exclude the presence of SC. Therefore, further analysis was carried out using X-ray photoelectron spectroscopy (XPS) and the results for both BNNS and GNP reported in **Figures 2** and **3**, respectively and, the main features summarized in **Tables 1** and **2**.

The XPS survey spectra of BNNS and the related treated materials display main peaks at 190.5, 397.5, 532.5, 284.5, and 1071 eV due to the atomic species B1s, N1s, O1s, C1s, and Na1s, respectively.[16] The ratio of B:N for the treated samples is not 1:1 as expected for a crystal of boron nitride (see untreated BNNS[16]), with a relative high nitrogen content. This result can be explained as follow; the cleaning procedures removed to some extent the impurities from the surface of the BNNS, forming highly unstable particles (unsaturated bonds) which are prone to degrade during EtOH washing and freeze drying, thus introducing defects in the crystal structure of BNNS, probably along the edges where erosion is more likely to occur.[16] The presence of oxygen, carbon, and sodium are impurities from the atmosphere (oxygen and carbon), some SC still present after the cleaning procedures and some ethanol for the EtOH-washed samples. The content of Na (from SC) in the freeze dried samples (both FD-(i) and FD-(ii)) is higher than for neat BNNS, probably due to the fact that the freeze drying is effective at separating the BNNS flakes, thus exposing larger areas of the samples covered with SC during the XPS measurements. In the case of the samples washed with ethanol, the sodium was completely absent, probably due to the ethanol being more effective at removing SC from BNNS. The higher resolution core-level photoemission spectra of B1s and N1s of the treated materials show asymmetric and broad peaks for all the BNNS samples studied, fitted by a combination of Lorentzian/Gaussian curves. The main peaks at 190 and 396.5 eV are due to the B—N bond for the B1s and N1s respectively, whereas the curves at 191.5 and 398 eV are due to the B—OH of B1s and N—H of N1s, respectively. The latter are associated with interactions between BNNS and SC and/or BNNS with ethanol in case of the EtOH-washed sample.[16] Additionally, the peak related to B—OH and N—H for all the treated samples are slightly shifted to lower binding energy compared to that for neat BNNS, probably due to a change in the electronegativity around the boron and nitrogen atoms after removing (at least partially) the impurities from the surface of the BNNS. It should be noted that some of the, oxidized groups on the BNNS surface could be a result of the exfoliation procedure of the bulk material.

The XPS survey spectra of the treated GNP samples identified the main peaks at 284, 532.5, and 1071 eV due to the atomic species C1s, O1s, and Na1s, respectively.[17] The presence of oxygen and sodium are due to impurities from both the atmosphere, SC and eventually ethanol from the EtOH-washed samples. The higher resolution core-level photoemission spectra of C1s shows asymmetric and a broad peak for carbon in all the GNP samples studied, as fitted by six Lorentzian/Gaussian combined curves. The main curve at 284 eV is due to C=C bonding, followed by C—C/C—H at 285 eV, C—O at 285.8 eV, C=O at 286.3 eV, O—C=O at 286.8 eV, and π–π^* at 290 eV.[25] The C—C/C—H, C—O, C=O, O—C = O bonds can be associated with the interaction between GNP and SC as well as with ethanol in case of the EtOH-washed samples.[17] As already observed for the BNNS spectra, the Na content of the freeze dried GNP samples (both FD-(i) and FD-(ii)) is higher than that for neat GNP, probably due to the exposure of larger areas of SC-covered GNP aggregates during the XPS measurement, as the GNP flakes separate during freeze drying. No shift in peak positions was detected for the treated materials with respect to neat GNP. Overall, the cleaning procedures did not change the electronegativity neighboring C1s, as the impurities (SC, traces of ethanol in the EtOH-washed sample) were not removed.

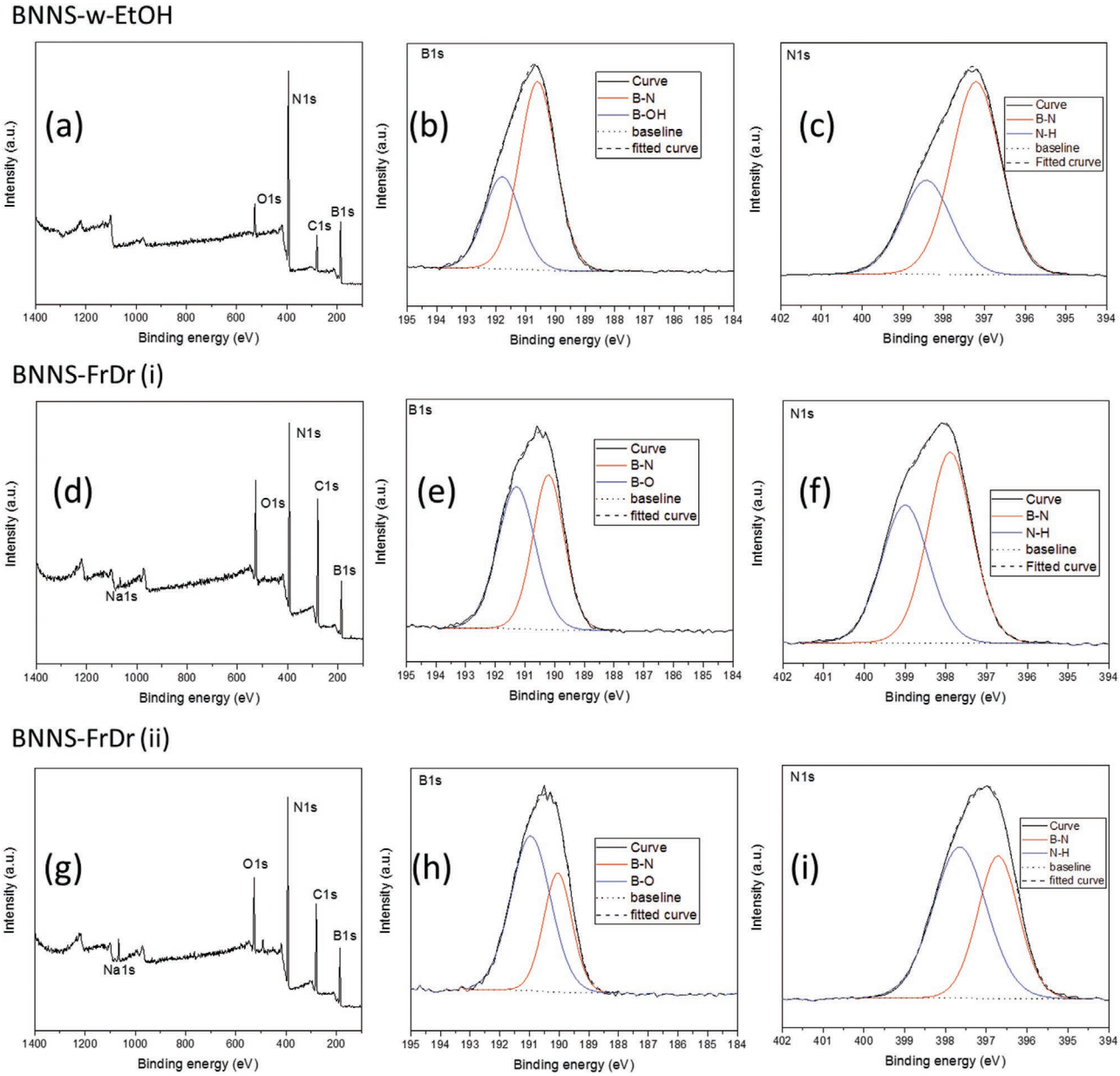

Figure 2. XPS results for treated BNNS: a,d,g) Survey spectra of BNNS-w-EtOH, BNNS-FD-(i), BNNS-FD-(ii), respectively; b,c) High resolution photoemission core spectra of B1s and N1s atoms respectively for the sample BNNS-w-EtOH. e,f) High resolution photoemission core spectra of B1s and N1s atoms for the sample BNNS-FD-(ii). h,i) High-resolution photoemission core spectra of B1s and N1s atoms for the sample BNNS-FrDr-(ii).

The thermo-gravimetric analysis (TGA) and DTGA (derivative of the weight loss) curves for the untreated and treated BNNS and, GNP are reported in **Figure 4**a,b.

The TGA curves of the BNNS and GNP before treatment show degradation at ≈400 and 600 °C, respectively. The TGA of the treated BNNS confirmed the total removal of water and no degradation occurred up to 800 °C under oxidative conditions. Similar results were obtained for the GNP samples post treatment, except for a slight amount of water still present in the GNP treated by freeze drying procedure FD-(i).

Figure 5 shows the X-ray diffraction (XRD) data for the treated BNNS and GNP samples relative to those untreated and the bulk materials that both are derived from, i.e., boron nitride (BN bulk) and graphite.

The XRD plots (Figure 5a) display the main peaks for BNNS before and after treatment at 2θ = 32°, 48.5°, 52°, 65° associated with the crystallographic planes (002), (100), (101), and (004), respectively. Both Bragg's law and Scherrer equations were applied on the peak (002) to characterize the crystalline structure of these materials (see also ref. [16]). From Bragg's law the interlayer distance d_{002} was calculated as 0.335 nm for both BNNS before and after treatment and from Scherrer's equation a value of L_{002} (thickness along the plane (002)) was estimated to be ≈2 nm for BNNS and ≈1.8 nm after

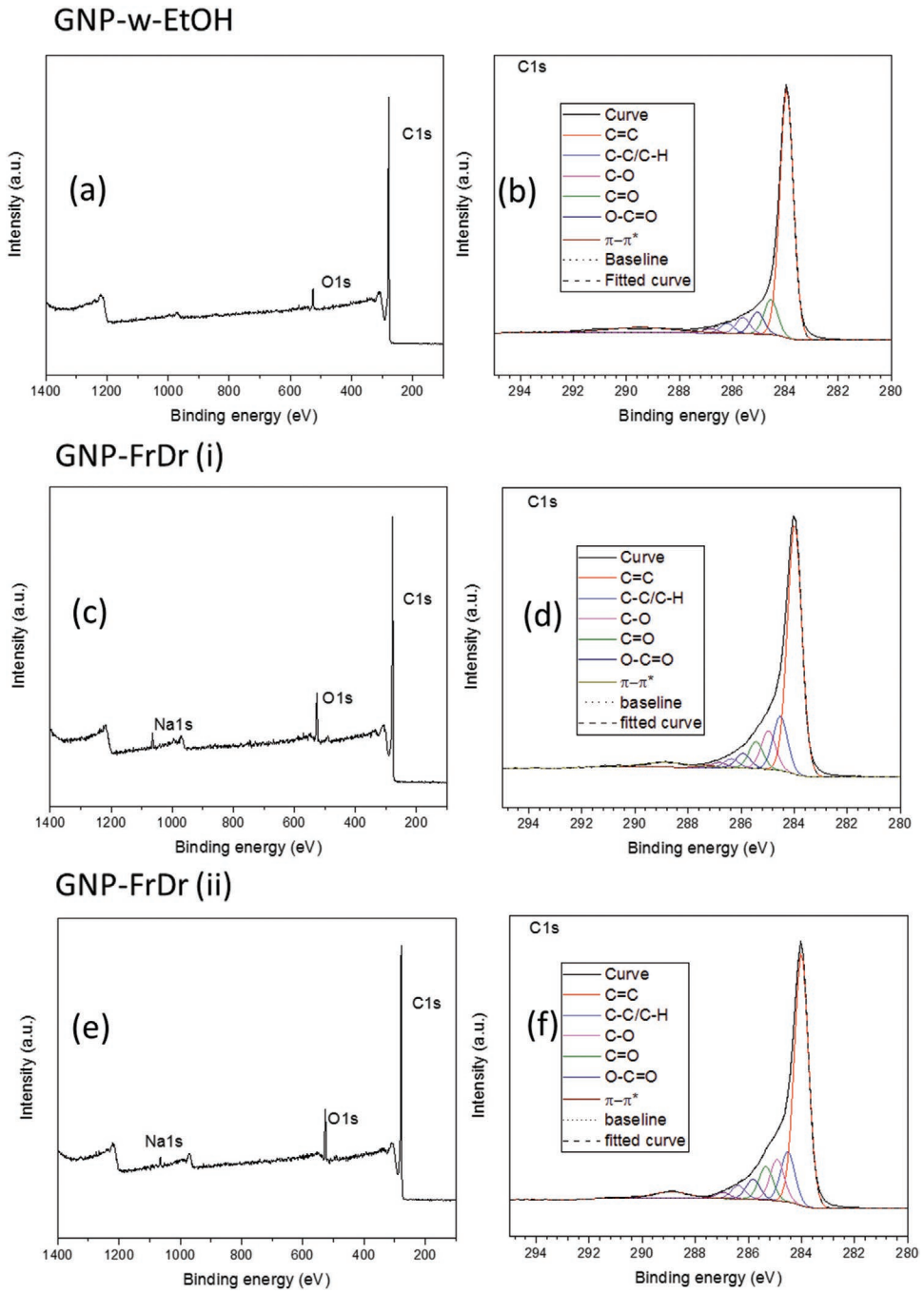

Figure 3. XPS results for treated GNP: a,c,e) Survey spectra of GNP-w-ETOH, GNP-FD-(i), GNP-FD-(ii), respectively; b,d,f) High resolution photoemission core spectra of C1s for the samples GNP-w-EtOH, GNP-FD-(i) and GNP-FD-(ii), respectively.

treatment. The application of Scherrer's equation to determine L_{002} should only be taken as an estimation since the equation is limited in application with materials having nanometer-scale dimensions. Indeed, the equation does not take into account the polydispersity of nanopowders.[26] Allowing for any error in the calculation and the validity of Scherrer equation on the nanometer-scale, the decrease of L_{002} for BNNS after treatment suggests that there may be separation of the BNNS aggregates along their thickness. However, since d_{002} does not change, the eventual separation occurs among different flakes stacked on top of each other and no exfoliation of the layers occurs as a consequence of the cleaning treatments. One of the possible reasons for the interflake separation in the BNNS may lie on the stabilizing effect of the surfactant SC diffused among the flakes during the preparation of BNNS from the BN bulk.

The XRD plots for GNP before and after treatment show the main peaks at $2\theta = 32°$, 48.5°, and 65°, due to the

Table 1. Summary of the XPS data for untreated BNNS and the respective treated materials. At(%) = atomic percentage of each atomic species detected. The table shows the assignment to the B1s and N1s peaks with the respective Lorentzian/Gaussian components.

Sample	At [%]	Main peaks	Lorentzian/Gaussian components
BNNS[16]	B: 20.3	190 eV	B*—N (190 eV)
			B*—OH (192.5 eV)
	N: 18.4	397.5 eV	B—N* (397.5 eV)
			N*—H (400 eV)
	C: 48	284.5 eV	–
	O: 13.2	532.5 eV	–
	Na: 0.05	1071 eV	–
BNNS-w-EtOH	B: 17	190.5 eV	B*—N (190 eV)
			B*—OH (191.5 eV)
	N: 61	397.5 eV	B—N* (396.5 eV)
			N*—H (398 eV)
	O: 12	532.5 eV	–
	C: 10	284.5 eV	–
BNNS-FrDr-(i)	B: 12	190.5 eV	B*—N (190 eV)
			B*—OH (191.5 eV)
	N: 39	397.5 eV	B—N* (396.5 eV)
			N*—H (398 eV)
	O: 20	532.5 eV	–
	C: 21	284.5 eV	–
	Na: 9	1071 eV	–
BNNS-FrDr-(ii)	B: 11	190.5 eV	B*—N (190 eV)
			B*—OH (191.5 eV)
	N: 36	397.5 eV	B—N* (396.5 eV)
			N*—H (398 eV)
	O: 27	532.5 eV	–
	C: 24	284.5 eV	–
	Na: 3	1071 eV	–

Table 2. XPS data for GNP and the respective treated materials. At(%) = atomic percentage of each atomic species detected. The table shows the assignment to the C1s peaks along with the respective Lorentzian/Gaussian components.

Sample	At [%]	Main peaks	Lorentzian/Gaussian component
GNP[17]	C: 90	284 eV	C=C (284 eV)
			C—C/C—H (285 eV)
			C*—O (285.8 eV)
			C*=O (286.3 eV)
			O—C*=O (286.8 eV)
			π–π* (290 eV)
	O: 9	532.5 eV	–
	Na: ≈1	1071 eV	–
GNP-w-EtOH	C: 90	284 eV	C=C (284 eV)
			C—C/C—H (285 eV)
			C*—O (285.8 eV)
			C*=O (286.3 eV)
			O—C*=O (286.8 eV)
			π–π* (290 eV)
	O: 10	532.5 eV	–
GNP-FrDr-(i)	C: 73	284 eV	C=C (284 eV)
			C—C/C—H (285 eV)
			C*—O (285.8 eV)
			C*=O (286.3 eV)
			O—C*=O (286.8 eV)
			π–π* (290 eV)
	O: 20	532.5 eV	–
	Na: 7	1071 eV	–
GNP FrDr-(ii)	C: 75	284 eV	C=C (284 eV)
			C—C/C—H (285 eV)
			C*—O (285.8 eV)
			C*=O (286.3 eV)
			O—C*=O (286.8 eV)
			π–π* (290 eV)
	O: 20	532.5 eV	–
	Na: 6	1071 eV	–

crystallographic planes (002), (100), and (004), respectively.[17] These plots were analyzed in the same manner as that for BNNS and similar observations made for GNP before and after treatment. The XRD data confirms that there could have been some flake separation but not exfoliation during the treatment of the BNNS and GNP.

From the results discussed above, the freeze-drying method FD-(ii) was as efficient as FD-(i) at removing water from the BNNS but even more efficient at removing water from GNP. Therefore, the BNNS and GNP samples post treatment using FD-(ii) were characterized further. **Figure 6** shows the Raman spectra of samples treated using FD-(ii) only.

The peak at 1360 cm^{-1} in Figure 6a is the characteristic Raman active vibrational mode (E_{2g}) of hexagonal BN. This peak is intense and narrow for as received BNNS but broad and asymmetric for BNNS after treatment. This may be due to both the quantum confined effect and Fano interaction.[27] The first is understood to originate from phonon scattering in nanocrystals (NS) whereas the second is related to electron-phonon scattering in NS.[27] When the NS decreases in size, the number of phonons participating in Raman scattering increases and a broad asymmetric peak results. Furthermore, according to Yogi et al.,[27] the higher the Fano interaction the broader and more asymmetric the Raman peak. Therefore, it is possible to speculate that the cleaning procedures adopted assisted the separation of BNNS agglomerates, which present layers of few nanometers in length (see ref.[16]), thus increasing the quantum confined effect and the Fano interaction.

The Raman spectra of GNP before and after treatment (Figure 6b) displayed six peaks at around 1350, 1580, 1650, 2450, and 2700 cm^{-1} due to D, G(E_{2g}), D′, G*, and 2D (G′) bands, respectively. The position and the intensity of the G band can give information as to the number of GNP layers. Usually, the intensity of this band increases linearly with the increasing

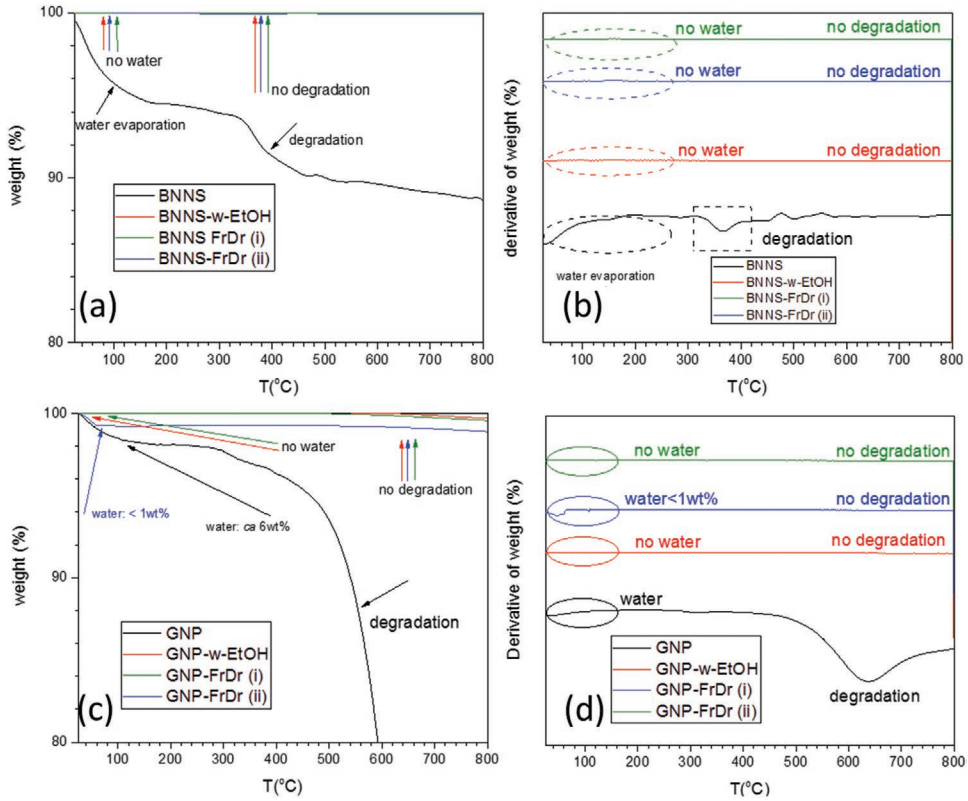

Figure 4. TGA curves (analysis performed under oxidative conditions) for a) untreated and treated BNNS, b) corresponding DTG curves for BNNS, c) TGA curves for untreated and treated GNP, and d) corresponding DTG curves for GNP.

number of layers and the peak shifts from 1587 (monolayer) to 1580 cm^{-1} (multilayer structure). In this case, the G band for the GNP is at 1580 cm^{-1} whereas post-treatment it is lower (≈1577 cm^{-1}), probably due to the agglomeration of GNP flakes after removing water.[17] These results highlight the challenge of cleaning the GNP surface without causing agglomeration of exfoliated flakes.

The intensity of the D and D′ bands are quite weak in all the spectra of the samples post treatment and similar to that before treatment suggesting a low defect concentration in the GNP crystal lattice which is unaffected by these treatment methods. The 2D band symmetry gives information about the number of GNP layers. A single layer produces a symmetric peak and the symmetry decreases with increasing number of layers.[17] For the treated GNP, the 2D band is slightly decentered and it is not particularly different from the 2D band of untreated GNP suggesting that no further exfoliation occurred as a consequence of the cleaning procedures used.

Compared to the treated BNNS, the treated GNP does not show any broadening or asymmetry of any peaks when compared with neat GNP. The difference between the two types of materials might be due to the size of the lateral dimensions of BNNS and GNP. The BNNS sheets (platelets) have nanometer-scale lateral dimensions whereas the GNP platelets have lateral

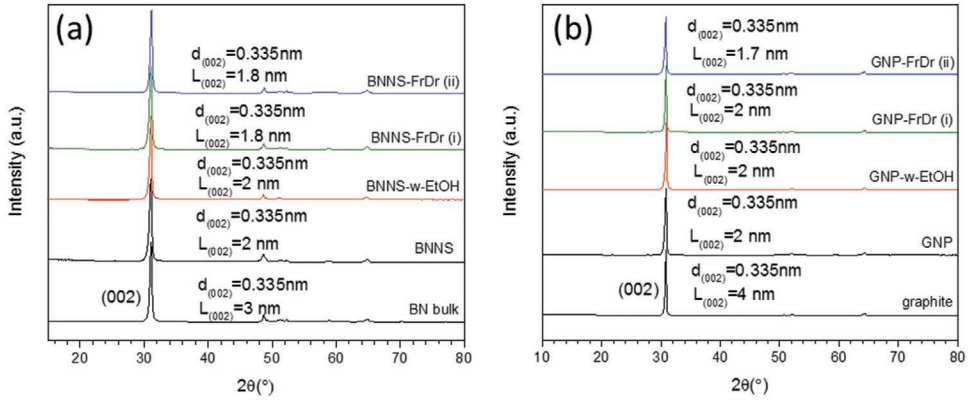

Figure 5. XRD pattern for a) BN bulk, BNNS, and treated samples and b) for graphite, GNP, and treated samples.

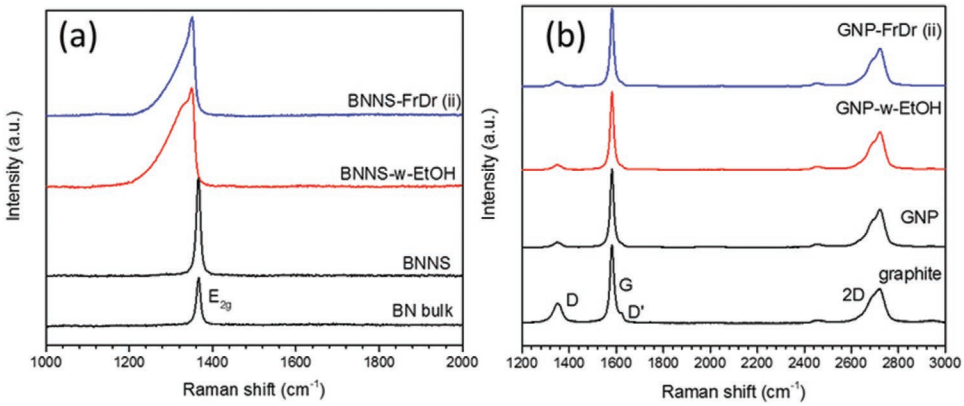

Figure 6. Raman spectra of a) bulk BN, BNNS, and treated BNNS materials and b) of graphite, GNP, and treated GNP materials, treatment using FD-(ii).

dimensions on the micrometer-scale (see ref. [17]), therefore the quantum confined effect and the Fano interactions (broadening and asymmetry of the Raman peak) in GNP are not as likely as in BNNS. Furthermore, the XPS results of the treated GNP suggest the cleaning procedures adopted did not actually remove impurities from GNP surface, thus, no evidence for changes to the lattice structure were detected.

The effect of application of FD-(ii) on the morphology of BNNS and GNP was examined by scanning electron microscopy (SEM) imaging the actual freeze dried-samples, see **Figure 7**.

As reported in our previous work,[16,17] BNNS and GNP agglomerates on the micrometre scale form layered structures. BNNS are round shaped platelets whereas GNP are more irregular square-shaped sheets see (insets in Figure 7a,b), respectively). The freeze-dried samples have similar morphology to the neat BNNS and GNP, although the BNNS flakes post treatment appear more separated than in neat BNNS and the surfaces imaged look smoother suggesting some cleaning has occurred.

3. Conclusions

Three procedures for the treatment of BNNS and GNP as a route to remove surface impurities (i.e., water, SC–ionic surfactant introduced during the exfoliation of bulk materials, i.e., boron nitride and graphite) during high-pressure homogenization are reported. These treatments included washing with ethanol (sample-w-EtOH), water assisted-freeze drying (FD-(i)), and freeze drying with no addition of water (FD-(ii)). FTIR spectroscopy proved the total removal of water from BNNS when treated using FD-(i) or FD-(ii), whereas some water (≈40%) and traces of ethanol were detected when BNNS was just washed with ethanol (BNNS-w-EtOH). This result was supported from TGA measurements, which also showed high thermal stability of the treated BNNS and GNP up to 800 °C under oxidative conditions. Results from XPS measurements did not allow for the total exclusion of the presence of SC in BNNS-w-EtOH and GNP-w-EtOH however, interesting insights in to the freeze-drying approach of the samples were discovered. In particular, the relatively high amount of sodium (from SC) in

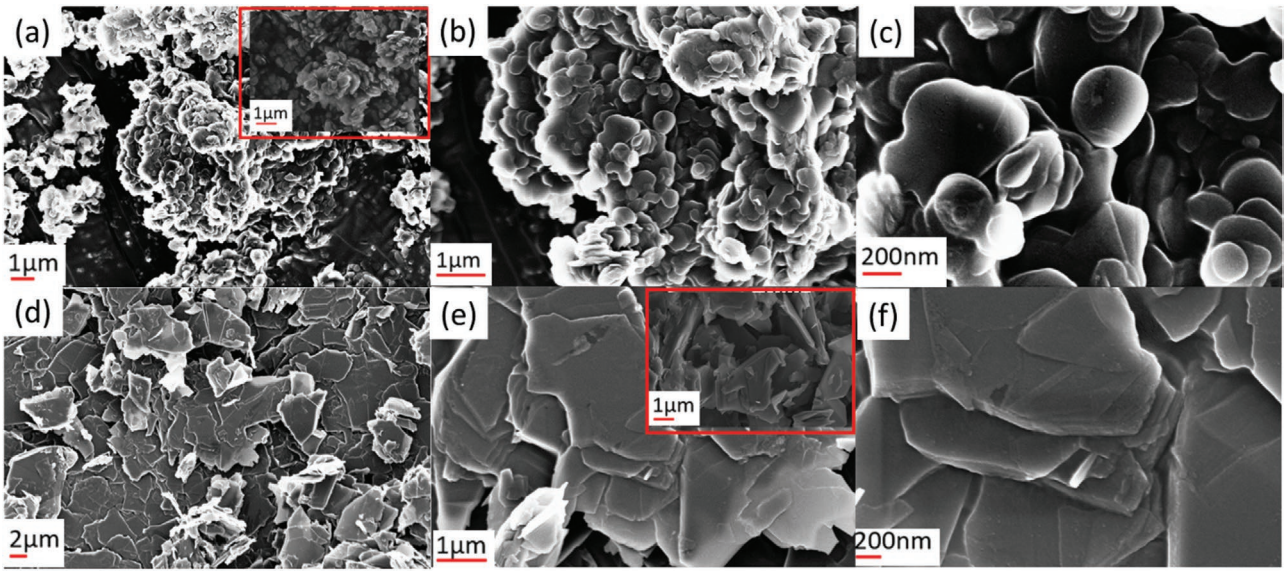

Figure 7. SEM images of a–c) BNNS-FD-(ii) and d–f) GNP-FD-(ii).

the BNNS/GNP-FD-(i) and BNNS/GNP-FD-(ii) suggest that freeze drying caused separation of BNNS and GNP aggregates to some extent. The XRD plots proved that the crystalline structure of BNNS and GNP was retained after treatment, whereas the Raman spectra revealed a broadening of the E_{2g} bands for BNNS-w-EtOH and BNNS-FD-(ii), due to both the quantum confined effect and Fano interaction, which originated from the separation of the nm length-scale flakes during cleaning. The Raman spectra of the GNP treated samples did not show any peak broadening, probably due to the large platelets (on the micrometer scale lateral dimensions) of the GNP compared to the BNNS, which results in a reduced quantum confined effect and Fano interaction for BNNS, thus peak broadening results. SEM imaging revealed a flake structure for both BNNS-FD-(ii) and GNP-FD-(ii) and the appearance of smoother surfaces.

In summary, washing with EtOH was more effective at removing SC from the surface of BNNS/GNP compared to freeze drying, but the latter is better for removing water. A disadvantage of using EtOH is that some solvent remains after treatment (see FTIR), the presence of which could affect BNNS/GNP dispersion in polymers, depending on the mixing method employed. There are also issues related to sustainability around using large amounts of solvent required for scale-up but, EtOH could be used as a precursor for the modification of the surface chemistry of BNNS/GNP. A disadvantage of using freeze-drying may be the cost related to the scale-up of the process.

4. Experimental Section

Materials: BNNS and GNP were kindly provided by Thomas Swan & Co. Ltd. and thoroughly characterized in our previous work.[16,17] BNNS and GNP were treated by washing with ethanol (EtOH) and freeze-dried using the following procedure—(1) Washing with EtOH was completed by diluting BNNS/GNP into EtOH (BNNS (GNP)/EtOH = 1g per 5mL) using a beaker and magnetic stirring for ≈15min. The suspensions of BNNS-w-EtOH and GNP-w-EtOH were then vacuum filtered and dried in an oven at 100 °C for 3–4 h. (2) Freeze drying was realized using two procedures; FD-(i)—diluting BNNS (GNP) in water (≈1g BNNS (GNP)/5 mL water) under magnetic stirring and freezing in liquid nitrogen until solidification of the dispersion before freeze drying. FD-(ii)—direct freezing in liquid nitrogen of BNNS (GNP) powder (≈20g of solid material placed in a beaker) and successive freeze drying as per FD-(i). The freeze-drying experiments were performed in the temperature range –15 to 0 °C at a pressure $\leq 10^{-3}$ bar using a Labconco FreeZone benchtop freeze dryer.

Characterization of BNNS and GNP Post-Treatment: The morphology of the materials after treatment was imaged using SEM with a Zeiss sigma field emission instrument. The imaging was performed with an InLens detector, a working distance of 3.2 mm and an acceleration voltage of 5 V. The samples (both powders) placed on aluminum stabs were covered with carbon tape and sputter coated with a Pd/Pt metal target (Cressington 108 auto) before imaging.

The crystalline structure of the samples was investigated by wide-angle X-ray diffraction (WAXD), using a PANalytical Empyrean X-ray diffractometer, fitted with a Co ($K_{\alpha 1}$ = 1.789 Å) source. The instrument was equipped with a PIXcel^{3D} detector, a tube voltage of 45 kV, and current of 40 A. The stage speed was set at 1rps and the experiments performed in reflectance mode.

FTIR measurements were carried out using a Bruker Spectrometer with a scan range between 500 and 4000 cm^{-1}. The samples all in powder form were, placed directly on the diamond crystal of the spectrometer and the spectra recorded in transmittance mode as an average of 34 scans.

TGA was performed using a Mettler Toledo TGA1-STARe to assess the thermal stability of the treated BNNS and GNP under oxidative conditions. The samples were heated from 25 to 800 °C at a constant heating rate of 10 K min^{-1}.

The lattice structures of the treated BNNS and GNP were studied using Raman spectroscopy with a Renishaw inVia Reflex confocal Raman microscope (Gonzo). The instrument was equipped with a 532 nm solid-state laser and ×5, ×20, ×50 objectives, a Renishaw CCD detector (Visible–NIR) and a 10 mW laser. The laser was spot focused on the samples with an exposure time of 2 min and five collections.

XPS measurements were performed to investigate the surface(s) of the treated BNNS and GNP using, a Kratos Axis Ultra delay-line-detector XPS, fitted with a magnetic immersion lens and charge neutralization system with spherical mirror and concentric hemispherical analyzers. The results from the measurements were analyzed using CasaXPS analysis software. The details of the instrument setup are reported in the previous work.[16,17]

Acknowledgements

V.G. thanks the Engineering and Physical Sciences Research Council (EPSRC) (Grant number EP/L016389/1) and Thomas Swan & Co Ltd for funding an EngD Studentship.

Conflict of Interest

The authors declare no conflict of interest.

Keywords

2D materials, boron nitride nanosheets (BNNS), exfoliated graphite nanoplatelets (GNP), surface cleaning

Received: May 27, 2020
Revised: July 20, 2020
Published online:

[1] Y. Kudo, K. Takai, T. Enoki, *J. Mater. Res.* **2013**, *28*, 1097.
[2] F. Giannazzo, S. Sonde, R. Lo Nigro, E. Rimini, V. Raineri, *Nano Lett.* **2011**, *11*, 4612.
[3] S. F. Chowdhury, S. Sonde, S. Rahimi, L. Tao, S. Banerjee, D. Akinwande, *Appl. Phys. Lett.* **2014**, *105*, 1.
[4] H. M. Lv, H. Q. Wu, K. Xiao, W. N. Zhu, H. L. Xu, Z. Y. Zhang, H. Qian, *Appl. Phys. Lett.* **2013**, *102*, 1.
[5] J. Moser, A. Barreiro, A. Bachtold, *Appl. Phys. Lett.* **2007**, *91*, 1.
[6] Y. C. Lin, C. C. Lu, C. H. Yeh, C. H. Jin, K. Suenaga, P. W. Chiu, *Nano Lett.* **2012**, *12*, 414.
[7] A. G. F. Garcia, M. Neumann, F. Amet, J. R. Williams, K. Watanabe, T. Taniguchi, D. Goldhaber-Gordon, *Nano Lett.* **2012**, *12*, 4449.
[8] F. A. Chambers, G. W. Zajac, T. H. Fleisch, *J. Vac. Sci. Technol., B* **1986**, *4*, 1310.
[9] P. Shrestha, M. T. Alkhafaji, M. M. Lukowitz, G. L. Yang, A. D. Migone, *Langmuir* **1994**, *10*, 3244.
[10] P. L. Fortucci, V. D. Meyer, E. K. Pang, *Anal. Chem.* **1985**, *57*, 2995.
[11] K. P. Loh, I. Sakaguchi, M. N. Gamo, S. Tagawa, T. Sugino, T. Ando, *Appl. Phys. Lett.* **1999**, *74*, 28.
[12] S. W. King, R. J. Nemanich, R. F. Davis, *Surf. Interface Anal.* **2015**, *47*, 798.
[13] S. Giljean, M. Bigerelle, K. Anselme, H. Haidara, *Appl. Surf. Sci.* **2011**, *257*, 9631.

[14] H. R. Thomas, S. P. Day, W. E. Woodruff, C. Vallés, R. J. Young, I. A. Kinloch, G. W. Morley, J. V. Hanna, N. R. Wilson, J. P. Rourke, *Chem. Mater.* **2013**, *25*, 3580.
[15] C. A. Joiner, T. Roy, Z. R. Hesabi, B. Chakrabarti, E. M. Vogel, *Appl. Phys. Lett.* **2014**, *104*, 223109.
[16] V. C. W. Guerra, J. Sloan, V. Degirmenci, D. Presvytis, T. McNally, *Nanoscale* **2018**, *10*, 19469.
[17] V. Guerra, C. Y. Wan, V. Degirmenci, J. Sloan, D. Presvytis, M. Watson, T. McNally, *J. Mater. Chem. C* **2019**, *7*, 6383.
[18] G. Lee, L. Paul, M. Ronan, **2017**, WO2017/064496 A1:1-11.
[19] H. F. Zhang, I. Hussain, M. Brust, M. F. Butler, S. P. Rannard, A. I. Cooper, *Nat. Mater.* **2005**, *4*, 787.
[20] S. M. Jung, D. L. Mafra, C. T. Lin, H. Y. Jung, J. Kong, *Nanoscale* **2015**, *7*, 4386.
[21] Y. W. Cao, J. C. Feng, P. Y. Wu, *Carbon* **2010**, *48*, 3834.
[22] X. L. Zeng, L. Ye, S. H. Yu, R. Sun, J. B. Xu, C. P. Wong, *Chem. Mater.* **2015**, *27*, 5849.
[23] X. L. Zeng, Y. M. Yao, Z. Y. Gong, F. F. Wang, R. Sun, J. B. Xu, C. P. Wong, *Small* **2015**, *11*, 6205.
[24] B. Singh, G. Kaur, P. Singh, K. Singh, B. Kumar, A. Vij, M. Kumar, R. Bala, R. Meena, A. Singh, A. Thakur, A. Kumar, *Sci. Rep.* **2016**, *6*, 1.
[25] L. Stobinski, B. Lesiak, A. Malolepszy, M. Mazurkiewicz, B. Mierzwa, J. Zemek, P. Jiricek, I. Bieloshapka, *J. Electron Spectrosc. Relat. Phenom.* **2014**, *195*, 145.
[26] H. Jensen, J. H. Pedersen, J. E. Jorgensen, J. S. Pedersen, K. D. Joensen, S. B. Iversen, E. G. Sogaard, *J. Exp. Nanosci.* **2006**, *1*, 355.
[27] P. Yogi, S. K. Saxena, S. Mishra, H. M. Rai, R. Late, V. Kumar, B. Joshi, P. R. Sagdeo, R. Kumar, *Solid State Commun.* **2016**, *230*, 25.